Factors controlling the thermoluminescence spectra of rare earth doped calcium fluoride

Y Wang, Y Zhao, D White, A A Finch, P D Townsend

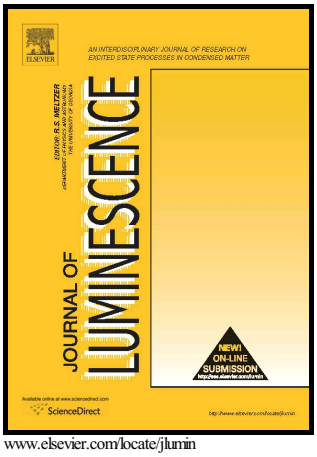

www.elsevier.com/locate/jlumin

PII: S0022-2313(16)31009-2
DOI: http://dx.doi.org/10.1016/j.jlumin.2016.12.011
Reference: LUMIN14426

To appear in: *Journal of Luminescence*

Received date: 31 July 2016
Revised date: 22 October 2016
Accepted date: 12 December 2016

Cite this article as: Y Wang, Y Zhao, D White, A A Finch and P D Townsend, Factors controlling the thermoluminescence spectra of rare earth doped calcium fluoride, *Journal of Luminescence* http://dx.doi.org/10.1016/j.jlumin.2016.12.011

Factors controlling the thermoluminescence spectra of rare earth doped calcium fluoride

Y Wang[1*], Y Zhao[1], D White[2], A A Finch[3], P D Townsend [4]

[1]School of Science, China University of Geosciences, Beijing, 100083, China

[2]Barnsley Hospital NHS Foundation Trust, Gawber Road, Barnsley S75 2EP, UK

[3]Department of Earth & Environmental Sciences, University of St Andrews, Fife, KY16 9AL, UK

[4]Physics Building, University of Sussex, Brighton, BN1, 9QH UK

*Corresponding author, wyfemail@gmail.com

Abstract

Thermoluminescence spectra of rare earth doped calcium fluoride samples, both powder and single crystal, were recorded over the temperature range from 25 K to 673 K. Although some broad band features exist, the spectra are dominated by the rare earth line transitions. The glow peak temperatures are slightly sensitive both to the ionic size of the dopants and the dopant concentration. By contrast, very considerable differences are generated by heat treatments, such as annealing followed by either fast or slow cooling. Comments are included on the reasons for such sensitivity in terms of association of dopant and intrinsic defect sites and why the results of dosimetry powder differ from those from single crystals.

Keywords: thermoluminescence, calcium fluoride, rare earth, ion-size

1. Introduction

Calcium fluoride (CaF_2) containing rare earth dopants has long been widely used in applications ranging from a scintillator lens [1], to a laser system [2], and as a radiation dosimetry material [3]. Recently, CaF_2 scintillator was also considered as a promising material applicable in physics for dark matter [4, 5]. Water Soluble CaF_2:Ln^{3+} nanocrystals have been prepared as a fluorescent labeling material for biology and clinical use [6]. Thus the ability to dope CaF_2 with rare earth ions has been widely exploited.

Despite the successful applications, the details of the way the rare earth ions are incorporated into the lattice are far less clear, and over time there have been a variety of ever more complex models. The changes in models partially reflect the fact that probably the first application of quantum mechanics was to calculate the energy levels of an electron in a box in an insulator, and relate the electronic states to the absorption properties of the F centres in alkali halides [7]. That was a simple system and the calculation was 90% successful. A closed box for a trapped electron is idealistic but evolving experimental techniques have detailed much longer range interactions, often extending over more than 50 shells of neighbouring ions [8-10]. Replacing a divalent calcium with a tri-valent rare earth ion demands some charge compensation, and also the mismatch in ionic volume introduces stresses. Typically, such stress can be reduced by association of defect complexes, and so the luminescence responses are sensitive not only to the chosen rare earth ion, but also the concentration of dopants, their association with intrinsic defects, and thermal processing treatments which allow aggregation or dissolution of complexes. For example, in an earlier study [11] of the spectra from Nd doped CaF_2, the thermoluminescence signals contained emission features characteristic of the Nd, but the isometric plots revealed dramatic changes with Nd concentrations of 0.01, 0.1 and 1.0 % of

Nd. That study, and others [12] indicate that the presence of Nd can quench intrinsic luminescence signals. Further, high temperature anneals at 500 ^{o}C followed by either slow or fast cooling, totally altered the precipitation of the associated Nd sites and thermally generated vacancies. Such effects are not unexpected, not least as at say a 1% dopant level, perfectly distributed Nd ions would be much less than 10 shells from another Nd ion (and this means they are not independent entities). The earlier Nd study was with single crystal material, whereas in many dosimetry systems powder samples are used, with powder sizes of perhaps 100 micron dimensions. In these situations, there is not only direct coupling between the rare earth dopants, but also perturbations from surface and intrinsic defects. Overall the expectation is that the thermoluminescence responses of crystalline material and powder will differ. Indeed, this is the case, and one of the current objectives is to investigate and contrast the TL responses with a number of rare earth examples, plus noting changes driven by heat treatments.

Rare earth (RE) ions modify the optical properties of CaF_2 since they strain and distort the original site symmetry, and require charge compensation. Such factors are reflected in optical properties such as the wavelength, line width, lifetime and relative intensity of the rare earth transitions [13] and the TL [14]. Other thermoluminescence examples have noted that rare earth dopants may even modify the overall lattice structure (i.e. not just the immediate neighbourhood of the dopant). Examples of total structural change are reported for ZnO and $SrTiO_3$ [15-17]. Inevitably such sensitivity exists as a function of the crystal supplier, grain size, ion type [18], concentration [19], impurities [13], method of excitation [20] and heat treatments to improve performance [21].

With such inherent complexity it is realistic to recognize that one may optimize performance

in applications, but rarely will one be able to have detailed knowledge of key lattice sites.

2. Experimental

Large single crystals of rare earth doped CaF_2 were obtained from Optovac (part of the Advanced Chemicals Division of EM Industries Inc). Thermoluminescence, photoluminescence and radioluminescence of these samples were recorded and described in an earlier doctoral thesis [22], some of these previously unpublished data are presented here.

The crystalline results are contrasted with new powder material grown for this study. The new samples include CaF_2: RE^{3+} (RE=Pr, Sm, Tb, Er, Dy, Ce) prepared by a high temperature solid-state reaction. According to the stoichiometric ratio, the raw material of $CaCO_3$, NH_4HF_2 and rare earth oxide were mixed in an agate mortar. The mixture was then placed in an alumina crucible and fired at 700 ^oC for 12 hours in the air. After cooling down over 4 hours, the fired samples were then ground into powder and prepared for the TL measurements. The rare earth ions doping concentration of the samples used in this work is 3wt%.

Thermoluminescence (TL) spectra, after X-ray irradiation, were obtained using a high sensitivity luminescence system [22, 23]. There are two temperature stages for the high and low temperature range. During the experiments, the high temperature stage operated from room temperature to 400 ^oC with a heating rate of 15 K/min. The irradiation dose was 40 Gy. The low temperature stage operated from 25 to 300 K after the samples was irradiated by X-rays at 25 K with a dose of 5 Gy. A low heating rate of 6 K/min was used so as to minimise the temperature lag between the sample and sample holder. Rapid heating results in major temperature gradients [24] and is inappropriate for the more fundamental investigations of the current work.

3 Results

3.1 Low temperature data

The current data are from an extensive total study of both crystal and powder samples, and therefore only a few selected figures are presented here. In all cases the rare earth ions introduce line emission spectra characteristic of the rare earth dopant. At low temperature the line spectra are the dominant features and broad band UV emission from the host lattice of CaF_2 is invariably weak or totally suppressed. This is consistent with earlier studies [11] in which the CaF_2 radioluminescence signals were proportionately reduced with increasing RE content. For single crystals there was also a definite pattern that the TL peak temperatures were displaced with changes in dopant concentration. Additionally, there were peak movements that are related to the ionic size of the rare earth. Both these features are consistent with other data of rare earth doping in insulating crystals, and for example have been reported with hosts of LaF_3 [25, 26] and $Bi_4Ge_3O_{12}$ [10]. For the CaF_2 host, increasing the dopant concentration tends to slightly lower the glow peak temperatures, and this trend extends from the lightly doped single crystal material to the more heavily doped powder.

Examples of the low temperature TL spectra are shown here as isometric plots of temperature, wavelength and intensity and/or as contour maps of the data. These figures are followed by a Table I which lists the main peak features seen in the various samples (both crystalline and powder).

Figure 1 is for Pr doped powder and here one observes the standard Pr emission lines in the TL emission, together with a weaker prolonged Pr signal over the entire temperature range. Very similar data were recorded below 100 K from single crystals with either 0.1% or 0.4% Pr doping levels. For the single crystals the minor feature near 150 K was absent. Figure 1 also includes a contour plot. Figure 2 has examples of isometric plots for Sm, Tb and Er, TL spectra from powder material. Note

that in the Sm data there is evidence for some broad band host TL at very low temperature. This behavior of low temperature intrinsic signals has also been noted elsewhere, as for the RE doping of LaF_3 and $Bi_4Ge_3O_{12}$. For Dy in CaF_2 the crystal the TL peaks are at a similar temperature, however, the pattern of relative intensities of the four strong lines is the reverse of that presented here for the powder. In our data from several different crystalline materials the relative line intensities vary with Dy content, but no obvious pattern has been identified. Nevertheless, for single crystal CaF_2 doped with either 0.1 or 1.0% Dy there is a reversal of the four-line intensity pattern compared with that from the powder. Figure 3 contrasts the low temperature Dy data from the powder with that from a single crystal with 0.1% Dy content. For the higher dopant level there are additional minor differences in the number of weak TL peaks.

Table I summarises the positions of the main TL peaks for rare earth doped CaF_2 both in single crystals and the powder samples. It is apparent that there are minor decreases in some of the peak temperatures with increasing dopant concentration. A similar pattern was observed in RE doped LaF_3 [25] where increasing dopant concentration lowered the peak temperature. For LaF_3 there was a clear trend relating the glow peak movement with size of the substituted rare earth ions. The changes matched both ion size and co-ordination number (despite the fact that there were indications that the dopants were in small related clusters) [25, 26].

Table I. Summary of low temperature TL peaks for rare earth doped CaF_2

Sample	Atomic number		Glow peak temperatures(K)			
Ce 0.1%	58		107	124	154	186
Ce (powder)	58	69				
Pr 0.1%	59	79	105	120	140	
Pr 0.4%	59	76		120	145	
Pr (powder)	59	75				
Nd0.01%	60	84	105	128	150	
Nd0.1%	60	85	106	127	147	181

Nd1.0%	60	82	109	130	148		
Sm (powder)	62	75					
Gd0.1%	64	79	106		147	181	249
Gd1.0%	64	84			148		
Tb (powder)	65	68					
Dy0.1%	66	85			148	181	
Dy 1.0%	66	82			148	171	
Dy (powder)	66	72					
Ho0.1%	67	88			151	187	247
Ho0.2%	67	82			147	181	243
Er0.1%	68	85	112		148	180	243
Er (powder)	68	71					

Figure 4 shows that for RE doped CaF_2 the low temperature peaks are very slightly shifted by the ion size, and the changes suggest a reduction in peak temperature with larger ions. The pattern extends up to Pr, at which point the Pr data are at noticeably lower values. The Pr ion is slightly smaller than the original Ca^{2+} ion, so this may minimize the lattice distortions. For the larger Ce ion the TL peak values have increased. This is not unexpected as the same pattern (but with much larger temperature movements) was noted in $Bi_4Ge_3O_{12}$ [10], with the lowest temperature value observed for ions of the size of the host site. Earlier views of such dependence were normally presented in terms of ionic radius, but since the lattice distortions are driven by changes of ionic volume the plot here is in terms of RE volume. The dotted lines are offered as a visual guide.

Table I lists the glow peaks detected at low temperature for the different rare earth dopants, but it does not indicate how they vary in relative intensity. Therefore, some TL responses are indicated by figure 5 for the powder material. To emphasize that powder and single crystal responses are not always identical figure 6 gives contour plots of Ce doped powder and crystal samples. For the crystal the lower temperature broad band signals may in part come from intrinsic TL. This possibility could explain why the signals move to longer wavelengths on heating (as the band gap decreases with temperature). However, there is a Ce^{3+} transition at 315 nm at room temperature, so the data may

merely be displaying how this highest level Ce transition is changing. The longer wavelength features are less temperature sensitive.

Rare earth dopants are characterized by their multiplicity of emission line, as seen for the RE luminescence transitions displayed in the TL data. The spectra recorded at low temperature for RE ions in CaF_2 often display only a limited number of strong features, figure 7, but include more signals at other wavelengths above room temperature. This pattern of behavior is repeated in many other insulators. In general, the long wavelength signals predominate at low temperature, but a more numerous set of lines are emitted at high temperature. Possible reasons are mentioned in the discussion.

3.2 High temperature data

Thermoluminescence above room temperature also shows the characteristic line spectra of the rare earth dopants but additionally there are a variety of broad emission bands. This is clearly evident in the case of Pr, as shown in figure 8. Similar mixtures of lines and bands are noted for Er, Dy and Ce, as seen in figures 9, 10 and 11. Broad bands are not necessarily linked to the RE dopants as the broad band features do not always occur at the same temperatures, either in terms of the RE signals, or between different samples with different RE dopants.

3.3 Effects of thermal treatments

In view of the previous examples of changing TL responses driven by thermal treatments some of the current samples were also thermally annealed to 500 ^{o}C and then either slowly or rapidly cooled. Modifications of the TL patterns were immediately obvious, both for the low and high temperature measurements. Figure 12 displays the high temperature contour plots for single crystals

of CaF_2: Er with a 0.1% erbium doping. Whilst the central line features are preserved, as well as two small emission bands near 400 and 660 nm, the patterns all differ, and visually one notes that there is no similarity in peak temperatures. In this figure the contrast is between data from the same crystal (a) as received; (b) after a 500 ^{o}C anneal followed by slow cooling and (c) after heating and thermally quenching. The main TL emission moved approximately from 150 to 225 to 200 ^{o}C. The signals appear with a pair of strong central lines at 525 and 537 nm (the resolution used here does not resolve finer details). The lines do not peak in the TL at identical temperatures and for figure 8 the values are (a) 155 and 150; (b) 228 and 222 and in (c) at 208 and 199 ^{o}C. A possible reason is included in the discussion.

As already mentioned, above room temperature such heat treatment effects had been noted previously in CaF_2 for Nd dopants of several concentrations. The present examples show that the emission patterns and glow peak temperatures are altered and figure 13 contrasts the high temperature TL for a crystal of CaF_2 with 0.1% Pr. The original signals from the 0.1% dopant level (figure 13a) differ from those with 0.4% Pr (figure 13b) where the lower temperature signals are missing. Heat treatments to 500 ^{o}C modify the pattern (figure 13c for the 0.4% Pr) but the change is independent of a fast or a slow cooling after heating.

4. Discussion

Rare earth doping of calcium fluoride produces thermoluminescence spectra with line emission features characteristic of the dopant ion. At low temperature the signals are predominantly from the rare earth ions with only minor traces of broad band luminescence that is characteristic of defects of the host material. By contrast, above room temperature many of the samples include a variety of line and broad band features. As indicated in the figures, the broad bands differ in both wavelength and

peak temperature from the rare earth signals, and indeed from material doped with different rare earth ions.

The rare earth ions vary in size from the calcium ion site that they occupy, and they also exist in a different charge state. The many consequences of these variations include the fact that the lattice is distorted, there is a need for charge compensating defects in the vicinity of the site and, as seen in earlier data for other material [10, 25-28], there is a high probability that the impurities will not be accommodated as individual dopants, but instead are likely to cluster in some fashion. The inherent consequences are that the defect structures and their stability (hence also the TL signals) will vary with (a) ion size, (b) dopant concentration and (c) thermal treatments which allow dissolution or clustering and production of intrinsic lattice vacancies. All three aspects are evidenced here (and elsewhere) for the TL for CaF_2 doped with rare earth ions.

The precision of the data is such that one is able to note small changes in the temperature of the low temperature TL peaks on changing dopant level, and an overall pattern is that the peaks appear at successively higher temperatures, depending on their divergence in size from the calcium site. With earlier data, from LaF_3 and bismuth germanate, the minimum TL value occurs for ions of the size of the host that has been replaced. This matches the example here for Pr doping that is a good match to the Ca ion size. However, for calcium fluoride the temperature shifts are small compared with those seen in the bismuth germanate or LaF_3.

Thermal treatments to alter association of impurities and defect sites are effective. The examples shown here at high temperature (for Er dopants figure 12, and for Pr in figure 13) indicate for Er a total trap depth restructuring between the original samples from those that were annealed and slow cooled and those annealed and thermally quenched. By contrast, above room temperature the Pr

data differ after annealing, but slow cooling and quenching produce similar responses. In all the higher temperature results there are a variety of broader line and band features that one assumes are linked to intrinsic defects, but there is no clear pattern how they relate to one another, or how the dopants are included. This mirrors the behavior of the earlier results for various Nd concentrations and thermal treatments.

There is an extensive literature that includes models of intrinsic defect sites in calcium fluoride [29, 30]. In earlier idealized models there are proposals for lattice vacancies at fluorine sites, and alternatives of rare earth charge compensation either by intrinsic defects or additional impurities. In irradiated material it had been assumed that the rare earth site was altered to a divalent state, so it could be accommodated in the host lattice. Such modelling had been fruitful in materials such as alkali halides, when the dopant and defect concentrations were sufficiently small (i.e. parts per million) that the defects were well separated. However, any attempt to link such modelling and speculations to the current rare earth doped systems (where dopant concentrations can be as high as 0.4%) is incredibly difficult. For the potential dosimeter materials the dopant levels are so high that the stability of the host lattice is completely undermined. This is not merely from the need for charge compensation, but also because of the close proximity of the dopant ions, and their intimate connections to charge compensators. Note that for the samples with a RE concentration of 0.4% (i.e.1 in 250 ions) it means in a perfectly dispersed system each RE ion is within ~7 lattice sites from another impurity ion. Further, original lattice ions are at half this distance from the impurities. This is not isolation, as site coupling at such short distances is well documented. The propensity to associate impurities to minimise the strain energy of the lattice will imply pairing and clustering (plus charge compensation) which results in large complex defect packages. This is a familiar situation in

dosimetry materials (e.g. in the TLD100) where each complex of trap and linked recombination site will involve associations and measurable lattice distortions spanning perhaps 20 or 30 host sites [31]). An extreme situation was noted in RE doped zircons [32] where the evidence suggests the dopant ions precipitate out into nanoparticles of an impurity phase.

One must note that in the heavily doped dosimetry powder the grain sizes are small (perhaps one hundred microns) and this offers an immense surface are that will both be distorted and provide bonding sites for atmospheric or other impurities, with all their associated strains and charge states. It is therefore not unexpected that, as seen here in CaF_2, there are measurable differences between the same dopants as recorded in dosimeter and single crystal material, and those where heat treatments have varied intrinsic defect concentrations. The problems of defect site modelling have been extensively mentioned by very many authors over the last quarter of a century [e.g 33].

Overall, the current data confirm that RE doping of calcium fluoride is an effective route for phosphors that will offer strong thermoluminescence for radiation dosimetry. Nevertheless, the design of such materials will continue to be empirical, as understanding the details of the impurities and lattice interactions is not realistic.

In terms of dosimetry efficiency, the association of traps and recombination sites is desirable as this provides a luminescence signal without competition from non-radiative sites (i.e. as in TLD100). Finding direct evidence for adjacent sites from luminescence data is unusual but several examples have been noted. In figure 12 it was seen that the green emission lines of the Er site have TL which is sensitive to thermal processing and, more critically, they differ in their TL peak temperatures by ~6 degrees. For long range separation of traps and recombination sites charge transport via the conduction band would not distinguish between the RE transitions. However, in closely linked sites

electron tunneling would initially favour the lower level transitions, as seen in this Er data. The same possibility has recently been reported for Tb and Eu doped magnesium orthosilicate dosimeters [34, 35] and a more general review includes examples from crystalline material [36]. The possibility of such tunneling has frequently been discussed but these RE emission spectra produce TL that offers direct evidence.

5. Conclusion

The complex thermoluminescence behavior from RE doping of calcium fluoride reveals the expected behavior of changes linked to impurity ion size, dopant concentration and defect associations controlled by heat treatments.

Acknowledgement

We would like to thank the support of the Fundamental Research Funds for the Central Universities of China (No.2-9-2015-191) and the National Nature Science Foundation of China (No.11205134).

References

[1] W. Hayes, Crystals with Fluoride Structure, Clarendon Press, Oxford, 1974.

[2] S. Kuck, Laser-related spectroscopy of ion-doped crystals for tunable solid-state lasers, Appl. Phys. B 72 (2001) 515-562.

[3] A.S. Pradhan, R.C. Bhatt, Some Parameters of Low and High LET Radiation Dosimetry using CaF_2:Tm TLDs, Radiat. Prot. Dosim. 6 (1-4) (1983) 175-177.

[4] Y. Shimizu, M. Mionwa, W. Suganuma, Y. Inoue, Dark matter search experiment with CaF_2 (Eu) scintillator at Kamioka Observatory, Phys. Lett. B 633 (2006) 195-200.

[5]I. Ogawa, T. Kishimoto, R. Hazama, S. Ajimura, K. Matsuoka, N. Suzuki, T. Nitta, H.

Miyawaki, S. Shiomi, Y. Tanaka, H. Ejiri, N. Kudomi, K. Kume, H. Ohsumi, K. Fushimi, Dark matter search with CaF_2 scintillators in Osaka, Nucl. Phys. A 663-664 (2000) 869c-872c.

[6] J. Wang, W. Miao, Y. Li, H. Yao, Z. Li, Water-soluble Ln^{3+}-doped calcium fluoride nanocrystals: Controlled synthesis and luminescence properties, Mater. Lett. 63 (2009) 1794-1796.

[7] R.W. Pohl, Electron conductivity and photochemical processes in alkali-halide crystals, Proc. Phys. Soc. 49 (4S) (1937) 3-31.

[8] B. Hayes, A.M. Stoneham, Defects and defect processes in nonmetallic solids Wiley, New York, 1985.

[9] P.D. Townsend, A.P. Rowlands, Extended defect models for thermoluminescence, Rad. Prot. Dosim. 84 (1999) 7-12.

[10] P.D. Townsend, A.K. Jazmati, T. Karali, M. Maghrabi, S.G. Raymond, B. Yang, Rare earth size effects on thermoluminescence and second harmonic generation, J. Phys.: Condens. Matter 13 (2001) 2211-2224.

[11] S.A. Holgate, T.H. Sloane, P.D. Townsend, D.R. White, A.V. Chadwick, Thermoluminescence of calcium fluoride doped with neodymium, J. Phys.: Condens. Matter 6 (1994) 9255-9266.

[12] N. Can, P.D. Townsend, D.E. Hole, H.V. Snelling, J.M. Ballesteros, C.N. Afonso, Enhancement of luminescence by pulse laser annealing of ion implanted europium in Sapphire and silica, J. Appl. Phys. 78 (1995) 6737-6744.

[13] M. Stef, A. Pruna, N. Pecingina-Garjoaba, I. Nicoara, Influence of Various Impurities on the Optical Properties of YbF_3-Doped CaF_2 Crystals, Acta Phyasica Polonica 112 (2007) 1007-1012.

[14] P.D. Townsend, D.R. White, Interpretation of rare earth thermoluminescence spectra, Rad. Prot. Dosim. 65 (1996) 83-88.

[15] Y. Wang, B. Yang, N. Can, P.D. Townsend, Indications of bulk property changes from surface ion implantation, Philos. Mag. 91 (2011) 259-271.

[16] B. Yang, P.D. Townsend, R. Fromknecht, Low temperature detection of phase transitions and relaxation processes in strontium titanate by means of cathodoluminescence, J. Phys.: Condens. Matter 16 (2004) 8377.

[17] Y. Wang, B. Ma, W. Zhang, D. Li, Y. Zhao, A.A. Finch, P.D. Townsend, Substrate lattice relaxations, spectral distortions, and nanoparticle inclusions of ion implanted zinc oxide, J. Appl. Phys. 118 (2015) 095703.

[18] M. Maghrabi, P.D. Townsend, Thermoluminescence spectra of rare earth doped Ca, Sr and Ba fluorides, J. Phys.: Condens. Matter 13 (2001) 5817-5831.

[19] J.J. Fontanella, M.C. Wintersgill, G.C. Kolodziejczak, D.R. Figueroa, C.G. Andeen, G.A. Royce, V.K. Mathur, R.J. Abundi, M.D. Brown, Radiation induced electrical relaxation in rare earth doped calcium fluoride, Nucl. Instr. Meth. Phys. Res. B 1 (1984) 431-435.

[20] A.K. Kleppe, P. Meissner, Investigations on Thermoluminescence and Phosphorescence Properties of Rare Earth Doped Calcium Fluoride, Radiat. Prot. Dosim. 88 (2000) 157-164.

[21] N. Can, P.D. Townsend, D.E. Hole, H.V. Snelling, J.M. Ballesteros, C.N. Afonso, Influence of pulsed laser annealing on rare earth implanted luminescence, Nucl. Inst. Methods B 113 (1996) 248-252.

[22] D.R.R. White, Spectral luminescence studies of rare earth doped CaF_2 and some synthetic Minerals, University of Sussex, 1995.

[23] B.J. Luff, P.D. Townsend, High sensitivity thermoluminescence spectrometer, Meas. Sci. Technol. 4 (1993) 65-71.

[24] A. Ege, Y. Wang, P.D. Townsend, Systematic errors in thermoluminescence, Nucl. Insts. Methods A 576 (2007) 411-416.

[25] B. Yang, P.D. Townsend, A.P. Rowlands, Low temperature thermoluminescence of rare earth doped lanthanum fluoride, Phys. Rev. B 57 (1998) 178-188.

[26] B. Yang, P.D. Townsend, Patterns of peak movement in rare earth doped lanthanum fluoride, J. Appl. Phys. 88 (2000) 6395-6402.

[27] T. Karali, A.P. Rowlands, P.D. Townsend, M. Prokic, J. Olivares, Spectral comparison of Dy, Tm and Dy/Tm in CaSO4 thermoluminescent dosimeters, J. Phys. D 31 (1998) 754-765.

[28] M. Maghrabi, T. Karali, P.D. Townsend, A.R. Lakshmanan, Luminescence spectra of CaSO4 with Ce, Dy, Mn and Ag codopants, J. Phys. D: Appl. Phys. 33 (2000) 477-484.

[29] E. Faulques, J. Wery, B. Dulieu, C. Seybert, D.L. Perry, Synthesis, fabrication, and photoluminescence of CaF2 doped with rare earth ions, J. Fluoresc. 8 (1998) 283-287.

[30] D.W. Mcmasters, B. Jassemnejad, S.W.S. Mckeever, Some observations regarding the effects of background rare-earth impurities on the thermoluminescence and optical absorption of CaF2:Mn, J. Phys. D: Appl. Phys. 20 (1987) 1182-1190.

[31] S.W.S. McKeever, M. Moscovitch, P.D. Townsend, Thermoluminescence dosimetry materials: Properties and uses, Nuclear Technology Publishing, Ashford, 1995.

[32] T. Karali, N. Can, P.D. Townsend, A.P. Rowlands, J. Hanchar, Radioluminescence and thermoluminescence of rare earth element and phosphorus-doped zircon, American Mineralogist 85 (2000) 668-681.

[33] F. Agullo-Lopez, C.R.A. Catlow, P.D. Townsend, Point Defects in Materials, Academic Press, London,1988.

[34] Y. Zhao, Y. Zhou, Y. Jiang, W. Zhou, A.A. Finch, P.D. Townsend and Y.Wang, Ion size effects on thermoluminescence of terbium and europium doped magnesium orthosilicate, J. Mater. Res. 30 (2015) 3443-3452.

[35] Y. Zhao, Y. Wang, M. Cui, H. Jin, Z. Fan, C. Zhao, X. Wu, P.D. Townsend, Morphology and thermoluminescence properties of terbium doped magnesium silicate, *submitted.*

[36] P.D. Townsend, A.A. Finch, M. Magrhabi, V. Ramachandran, G.L. Vazquez, Y. Wang, D.R. White, Nanoparticle and orbital effects in thermoluminescence, *in preparation.*

Figure 1. Low temperature isometric and contour plots of the TL of Pr doped CaF_2 powder samples.

Figure 2. Low temperature isometric plots of the TL of Sm, Tb and Er doped CaF_2 powder samples.

Figure 3. (a) A low temperature isometric plot of the TL of Dy doped CaF_2 powder sample. This is contrasted with that from a crystal of CaF_2 doped with 0.1% Dy.

Figure 4. Glow peak temperature in CaF_2 as a function of the volume of the RE dopant ions.

Figure 5. Integrated glow curves for doped CaF_2 powder.

Figure 6. (a) A contour plot for Ce doped CaF_2 powder; (b) TL contour map for a Ce doped CaF_2 crystal.

Figure .7 Examples of spectra from different RE dopants in CaF_2 powder.

Figure 8. TL above room temperature for Pr doped CaF_2 powder.

Figure .9 TL above room temperature for Er doped CaF_2 powder.

Figure 10. TL above room temperature for Dy doped CaF_2 powder.

Figure 11. TL above room temperature for Ce doped CaF_2 powder.

Figure 12.Varations in the high temperature TL of the same Er doped CaF_2 single crystal. The contours were (a) the original sample; (b) after annealing at 500 ^{o}C and slow cooling, whereas in (c) there had been rapid cooling.

Figure 13. Examples of high temperature with crystal containing Pr. (a) is for a crystal of CaF_2 with 0.1% Pr; (b) with 0.4% Pr and (c) after heat treatments to 500 ^{o}C for the same crystal.

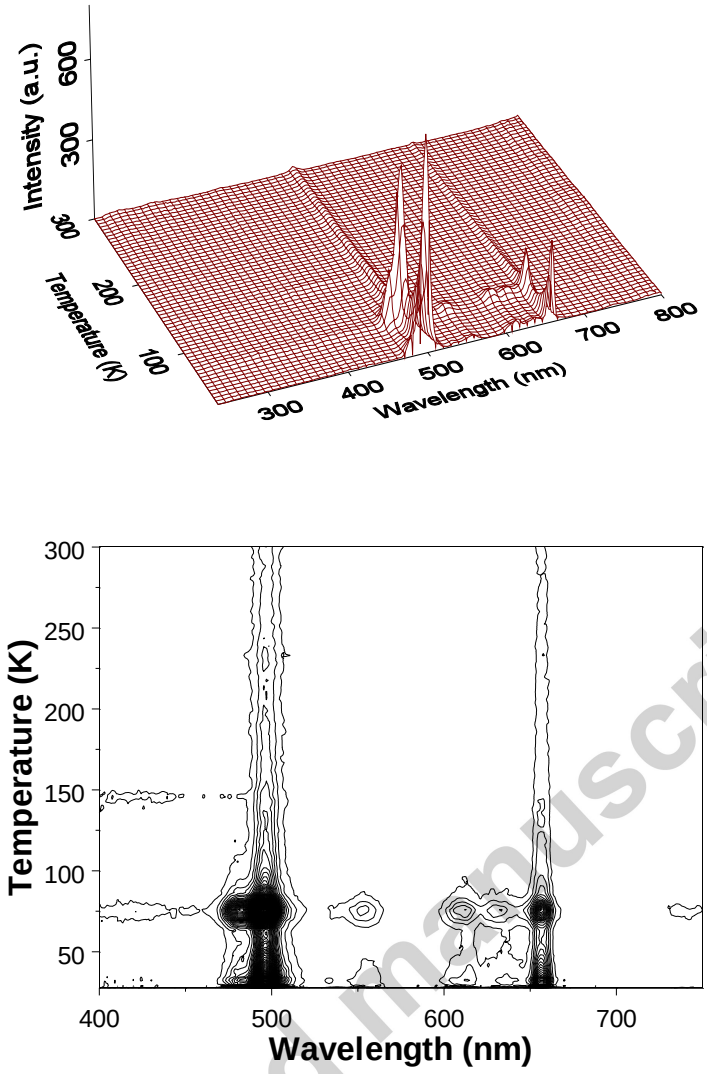

Figure1

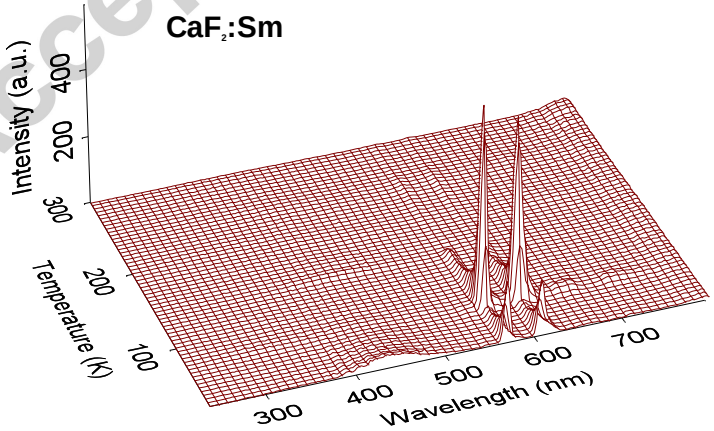

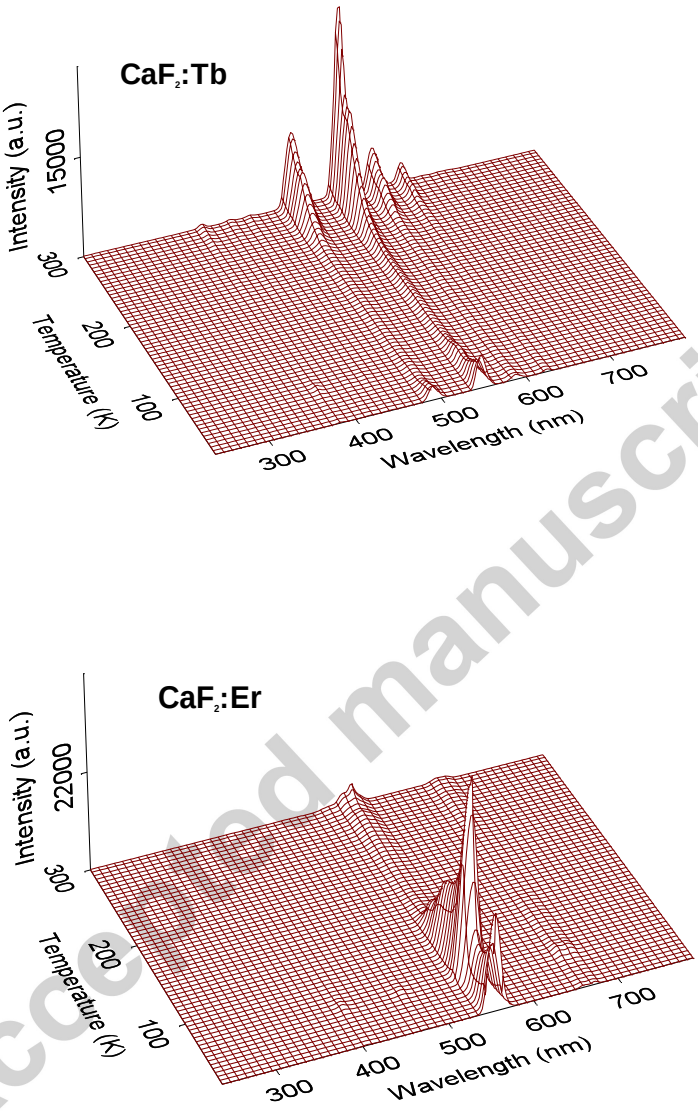

Figure2

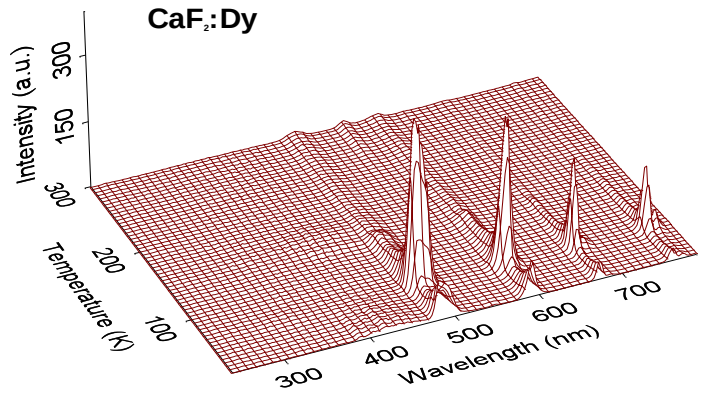

Figure3a

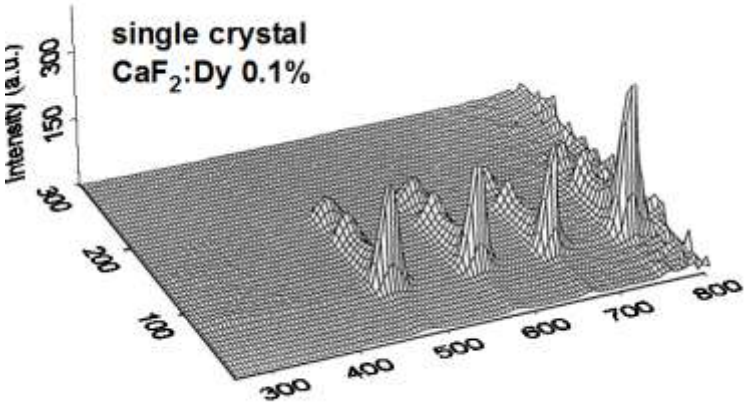

Figure3b

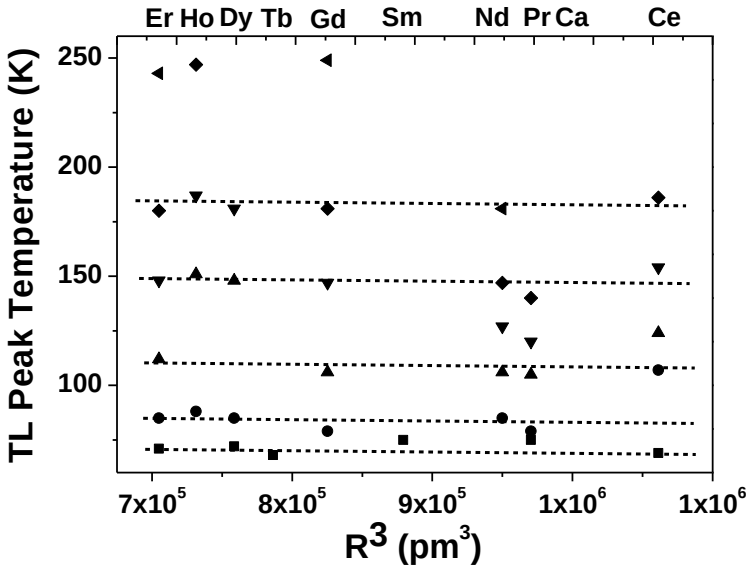

Figure 4

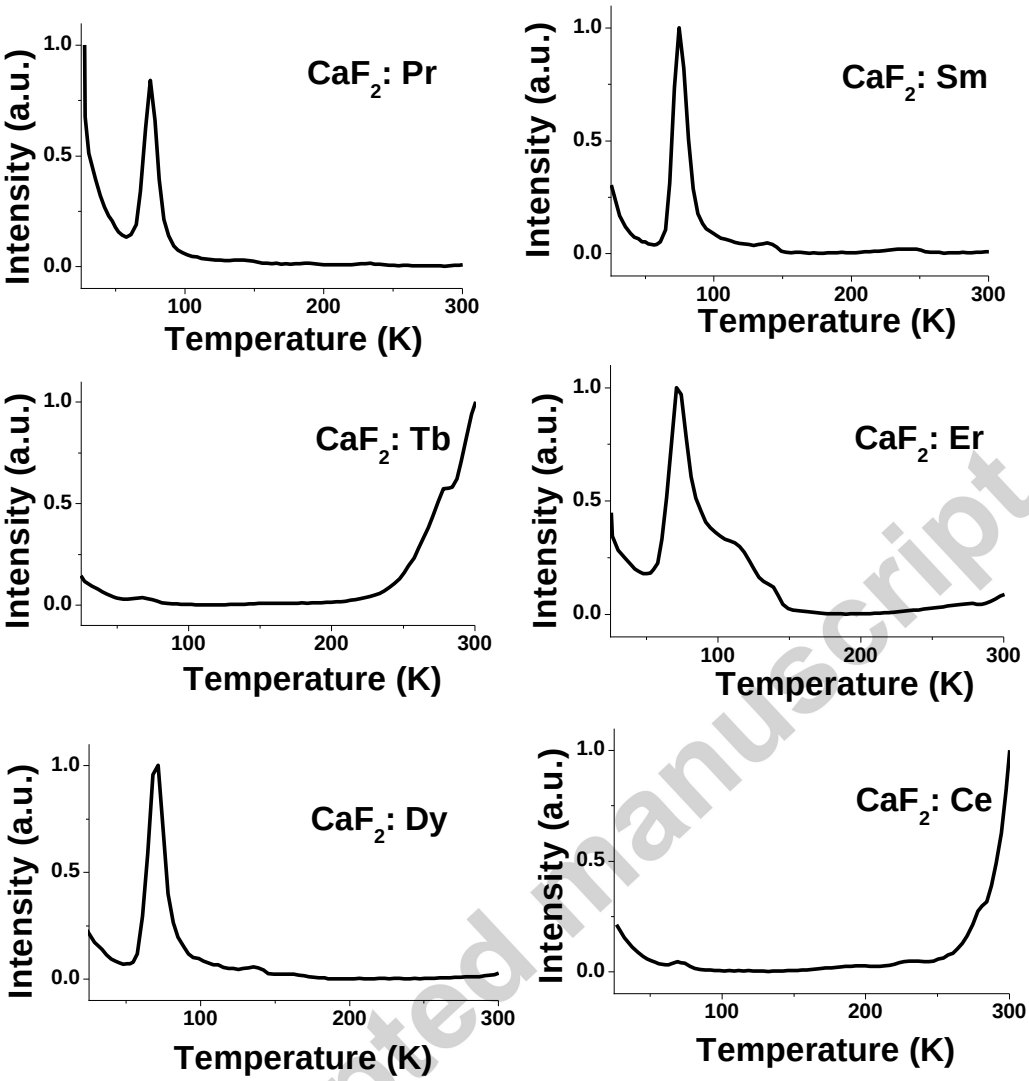

Figure 5

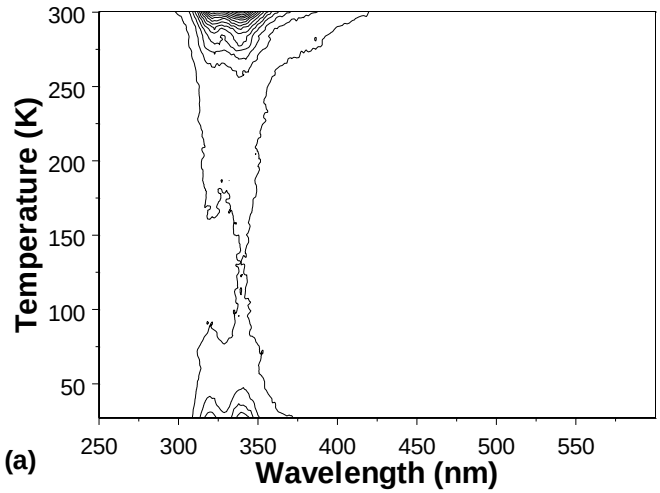

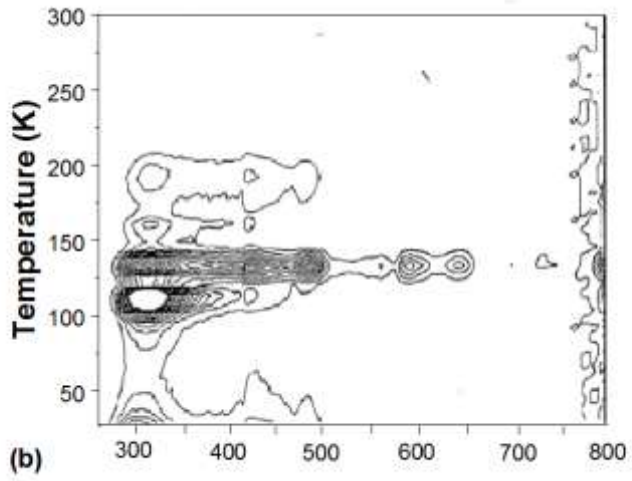

Figure 6

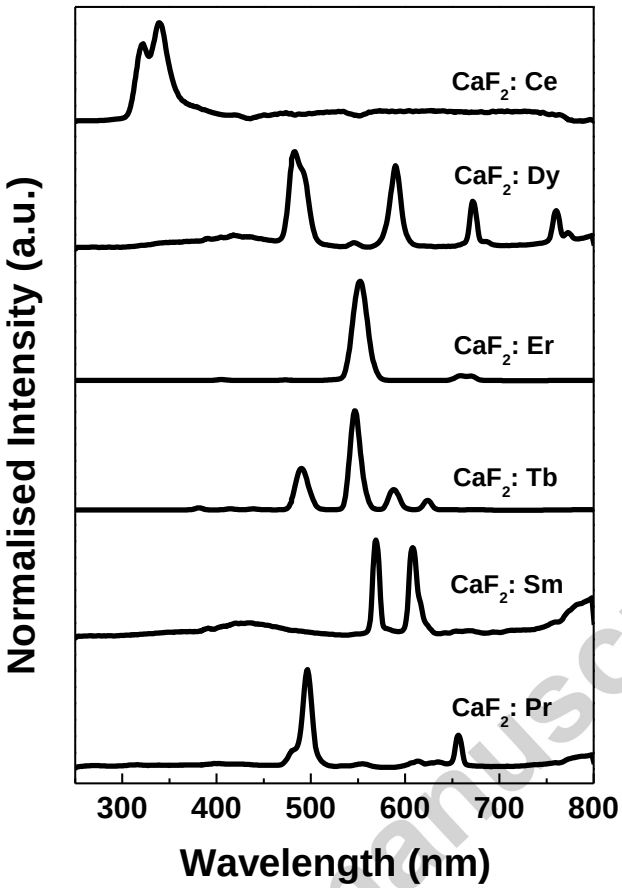

Figure 7

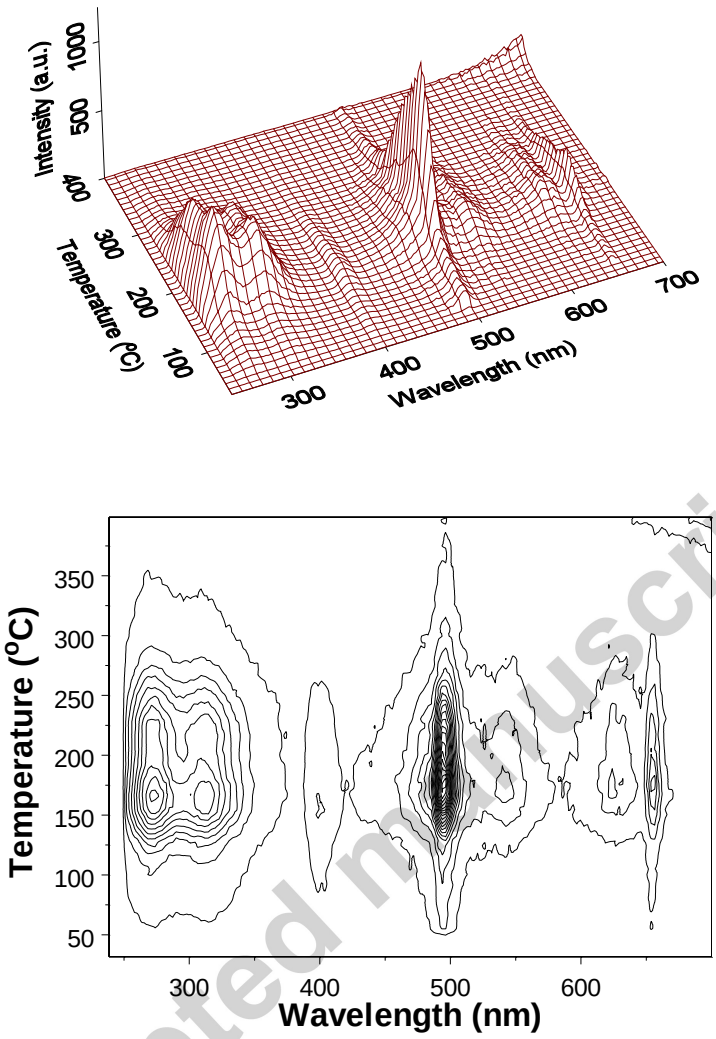

Figure 8

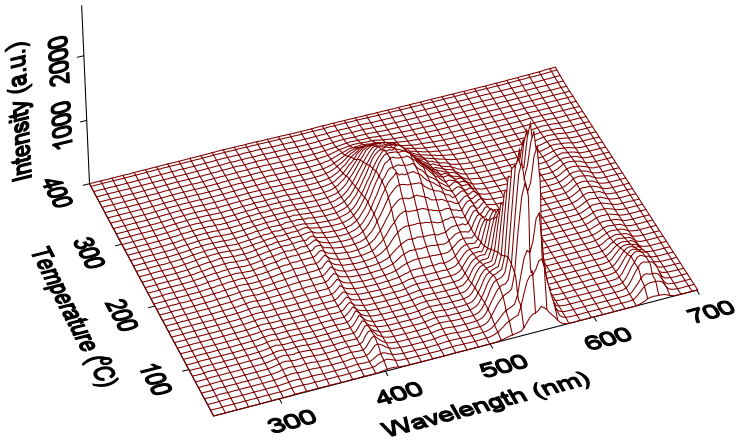

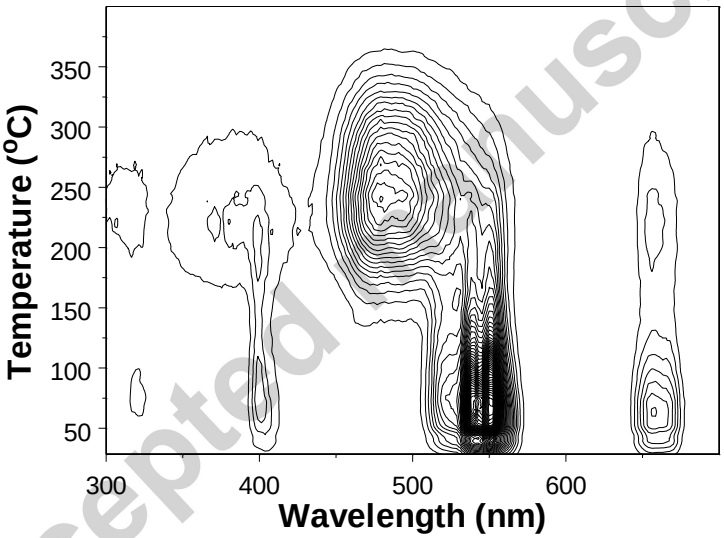

Figure 9

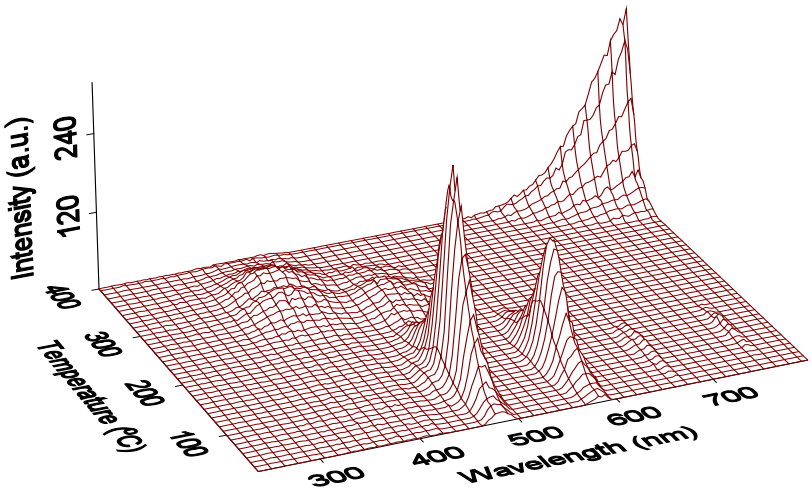

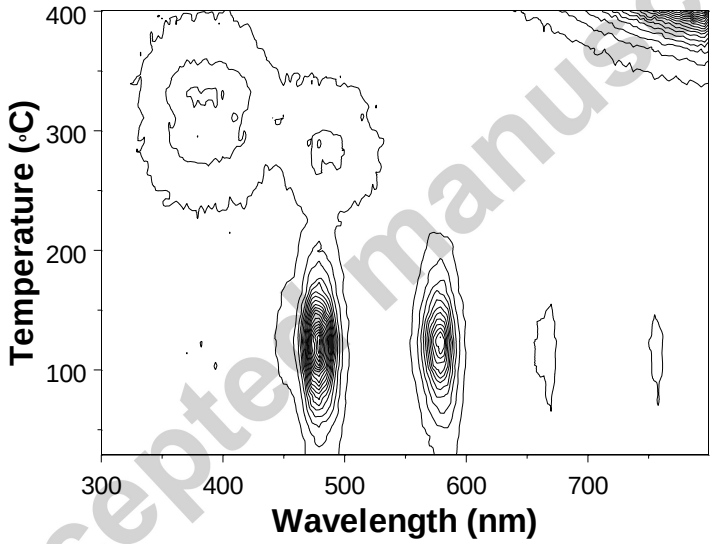

Figure 10

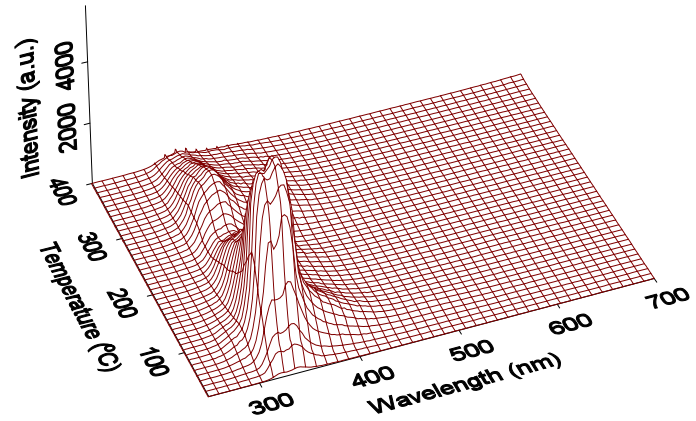

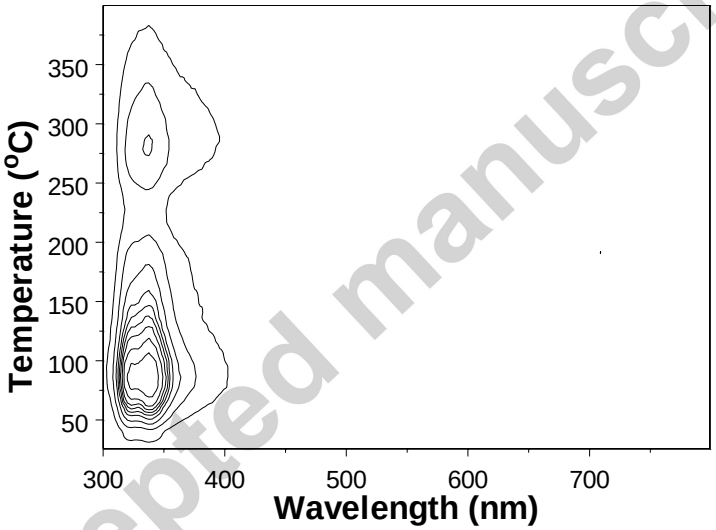

Figure 11

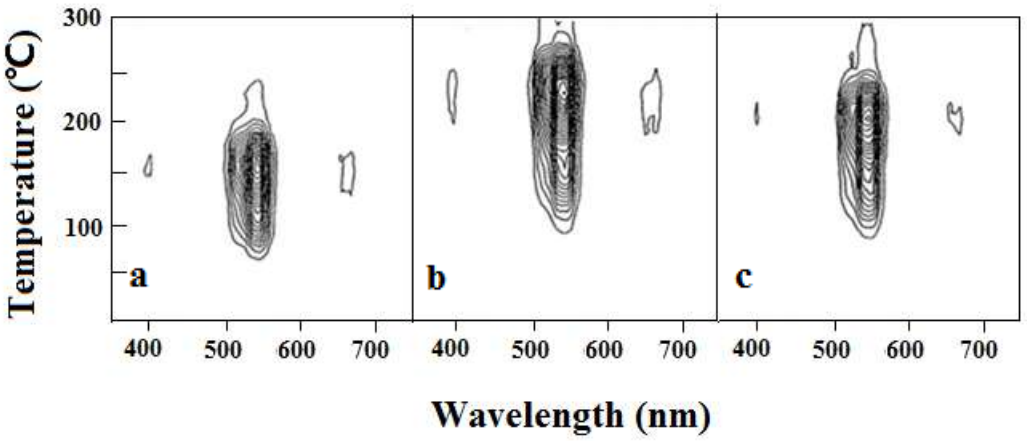

Figure 12

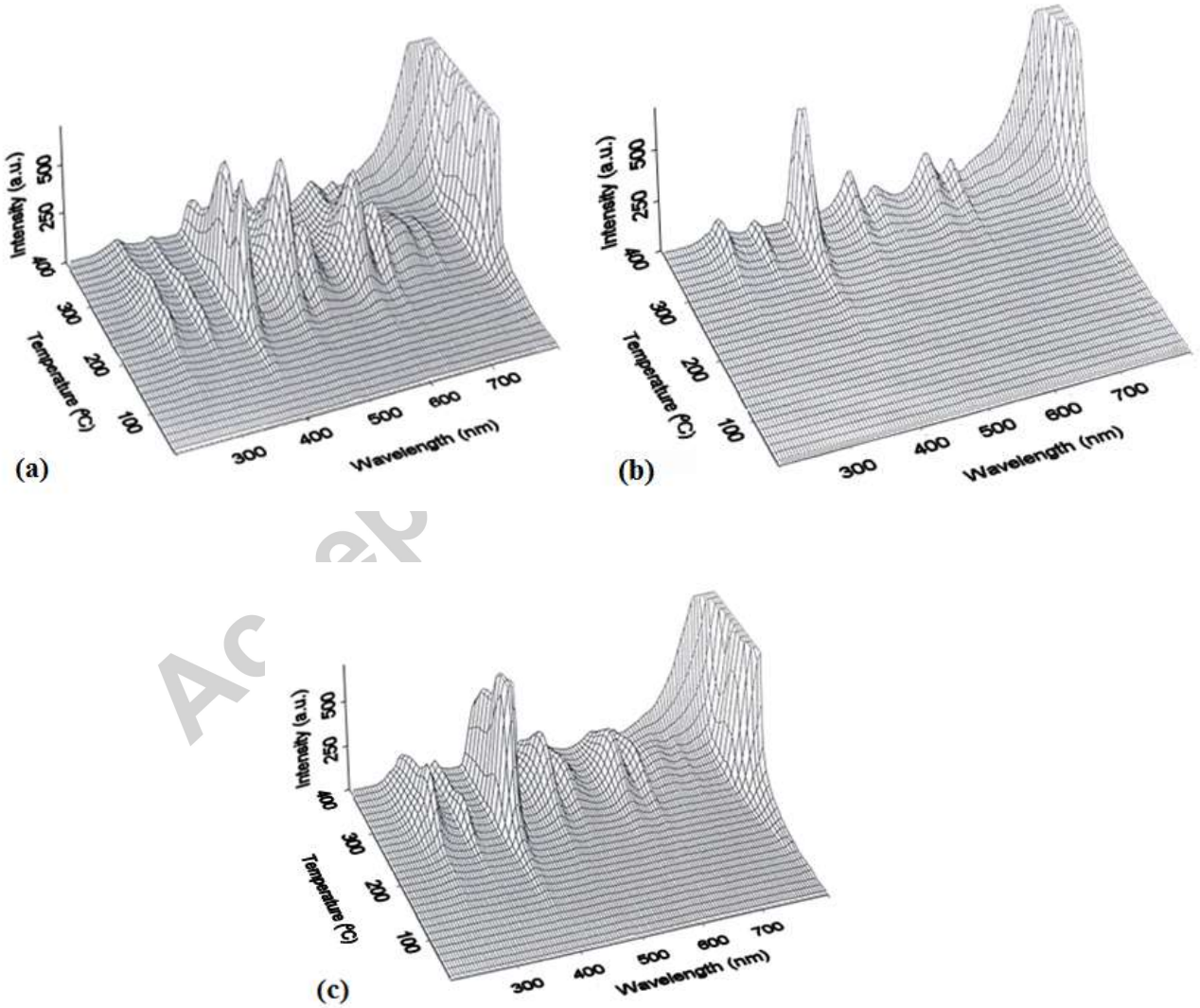

Figure 13